Failure of Russell-Saunders Coupling in the 5*f* States of Plutonium

K. T. Moore,[1,*] M. A. Wall,[1] A. J. Schwartz,[1] B. W. Chung,[1] D. K. Shuh,[2] R. K. Schulze,[3] and J. G. Tobin[1]

[1]*Lawrence Livermore National Laboratory, Livermore, California 94550, USA*
[2]*Lawrence Berkeley National Laboratory, Berkeley, California 94720, USA*
[3]*Los Alamos National Laboratory, Los Alamos, New Mexico 87545, USA*

(Received 17 January 2003; published 16 May 2003)

Using high energy–electron energy loss spectroscopy, transmission electron microscopy, and synchrotron-radiation-based x-ray absorption spectroscopy, we provide the first experimental evidence that Russell-Saunders (*LS*) coupling fails for the 5*f* states of Pu. These results support the assumption that only the use of *jj* or intermediate coupling is appropriate for the 5*f* states of Pu. High energy–electron energy loss spectroscopy experiments were performed by use of a transmission electron microscope and are coupled with image and diffraction data; therefore, the measurements are completely phase specific.

DOI: 10.1103/PhysRevLett.90.196404 PACS numbers: 71.27.+a, 71.10.–w

The nature of Pu 5*f* electronic structure is still under debate [1–7]. Many of the complications are derived from the necessity of explaining the phase-specific behavior of Pu and Pu alloys, particularly the low-symmetry monoclinic α phase and the high-symmetry fcc δ phase. Experimentally, there are severe impediments, such as the present inability to grow large single crystals and the radioactive and chemical hazards of the materials. Theoretically, electronic structure calculations that have turned out reliable for all other metallic systems have failed for Pu because the 5*f* electrons are on the borderline between localized and itinerant behavior. Recent advances, including the application of dynamical mean-field theory to δ-Pu [2] and generalized gradient approximation to δ-Pu [3] and to α-Pu and δ-Pu [4], have begun to pave the way to better understanding of Pu 5*f* electronic structure. However, despite these efforts and earlier theoretical treatments [8], there is still a considerable lack of experimental data to support assumptions made in the computational framework. One of these critical issues is the degree to which the interaction of the spin and orbital angular momenta in the 5*f* states must be included in such calculations.

In the foundation of each of the above models [2–4] there are two limiting cases for the coupling of angular momenta in multielectronic systems: Russell-Saunders (*LS*) coupling and *jj* coupling. For a simple, two-electron system, these can be expressed as shown in Table I [9]. For atoms where the spin-orbit coupling is weak, the interactions between the orbital angular momenta of individual electrons is stronger than the spin-orbit coupling between the spin and orbital angular momenta. It can be assumed that the orbital angular momenta of the individual electrons add to form a resultant orbital angular momentum L, and that the individual spin angular momenta add to form a resultant spin angular momentum S. L and S are then summed to form the total angular momentum J. For heavier elements with larger nuclear charge, spin-orbit interactions begin to overshadow the interactions between individual spins or orbital angular momenta. Therefore, the spin and orbital angular momenta of each electron couples to form individual electron angular momenta. These individual electron angular momenta, $j_1, j_2, j_3, \ldots$, are then summed to give the total electron angular momenta J.

Historically, the Russell-Saunders approach has been shown to be generally highly successful with the rare earths [10], and because of this early modeling of actinides was based on a nonrelativistic approach, i.e., neglecting spin-orbit splitting [5]. However, over the last 20 years calculations have shown that there should be a considerable spin-orbit split in the 5*f* states of the actinides and that *jj* or intermediate coupling schemes more accurately match the behavior of such metals [8]. In this Letter, we present the first experimental evidence for the failure of Russell-Saunders coupling in the 5*f* states of plutonium via the absence of prepeak structure at energies below the main continuum peak of the $O_{4,5}$ absorption edge of plutonium.

High energy–electron energy-loss spectroscopy (HEEELS) results acquired using a transmission electron microscope (TEM) are shown for α-Th, α-U, α-Pu, and δ-Pu in Fig. 1. The Th and U samples were produced at the Ames Laboratory and at Oak Ridge National Laboratory, respectively, each of which was at least 99.9% pure. The Pu sample was an alloy with dilute Ga doping and contained a two-phase mixture of α and δ. The α phase was

TABLE I. *LS* versus *jj* coupling: for two particles (1,2) and four angular momenta (l_1, l_2, s_1, s_2).

LS	*jj*
$L = l_1 + l_2$	$j_1 = l_1 + s_1$
$S = s_1 + s_2$	$j_2 = l_2 + s_2$
$J = L + S$	$J = j_1 + j_2$

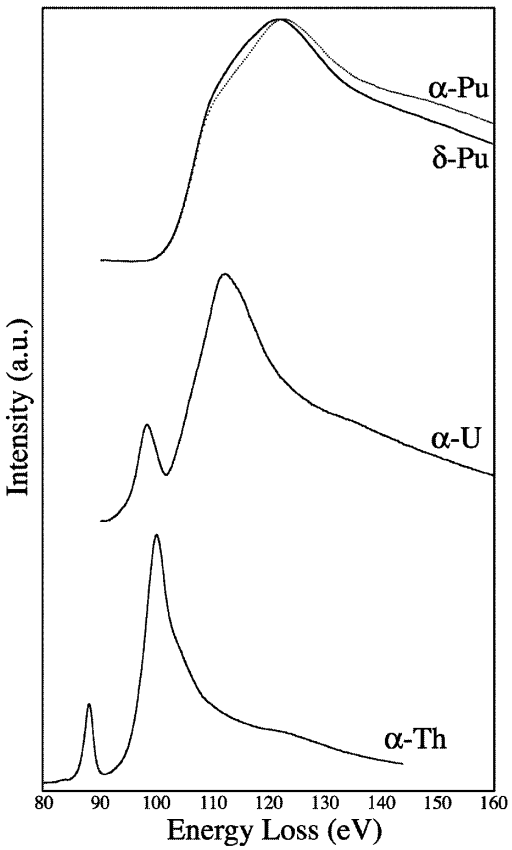

FIG. 1. The $O_{4,5}$ ($5d \rightarrow 5f$) HE-EELS edges from α-Th, α-U, α-Pu, and δ-Pu acquired by use of a TEM. These spectra were collected at an accelerating voltage of 297 keV and an energy resolution of 0.8 eV.

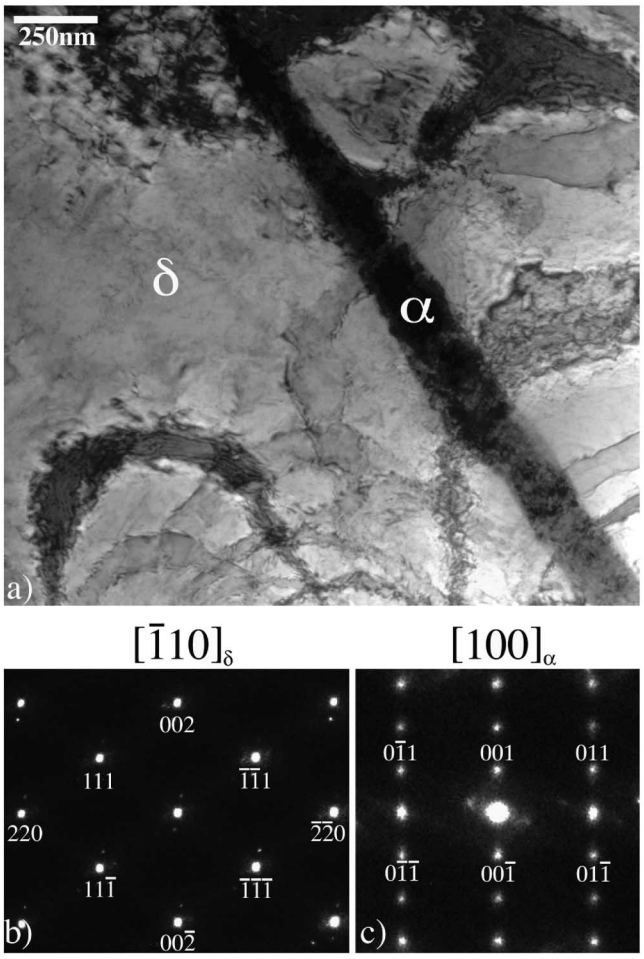

FIG. 2. (a) A bright-field TEM image acquired near a $[\bar{1}10]_\delta \| [100]_\alpha$ zone axis showing an α plate in a δ matrix. (b) A $[\bar{1}10]$ diffraction pattern from δ and (c) a [100] diffraction pattern from α, each with a number of reflections indexed.

formed by cooling a sample of pure δ phase to 153 K for 10 h, causing a $\delta \rightarrow \alpha$ martensitic phase transformation. Since the $\delta \rightarrow \alpha$ phase transformation was martensitic, i.e., diffusionless, both phases had identical composition.

A TEM provides the capabilities of imaging and diffraction, which ensures HE-EELS spectra are acquired from a single phase. The ability to differentiate the α and δ regions of Pu is illustrated in Figs. 2(a)–2(c). A two-phase mixture of α-Pu and δ-Pu is shown in the bright-field image in Fig. 2(a), where an α plate is the dark band contained in the surrounding bright δ matrix. Diffraction patterns acquired from a single-crystal area of δ and α are shown in Figs. 2(b) and 2(c), respectively. A field-emission-gun electron source, such as the one used in these experiments, can produce an electron probe small enough to record spectra and diffraction patterns from an area with a radius of 5 Å. Upon examination of the scale bar in Fig. 2(a), it is obvious that the problem of sampling multiple phases when recording spectra is alleviated. Furthermore, HE-EELS in a TEM is bulk sensitive, and the electron transitions are justified as dipole because the primary energy of the electron beam is 297 kV, much larger than the energy of the $O_{4,5}$ transitions for Th, U, and Pu [11]. There was a small amount of oxide on the surface of the TEM samples, but it was insignificant in comparison to the approximately 50 nm of metal sampled through transmission of the electron beam.

The salient feature of the $O_{4,5}$ HE-EELS edges in Fig. 1 is the disappearance of the small prepeak below the main continuum peak when moving along the $5f$ series from α-Th to α-U to α-Pu and δ-Pu. This is direct evidence for the necessity of jj coupling in Pu, since the absence of a prepeak correlates to the filling of the $5f^{5/2}$ sublevel in the $5d^{10}5f^5 \rightarrow 5d^9 5f^6$ transition.

Synchrotron-radiation–based x-ray absorption spectroscopy (XAS) and photoelectron spectroscopy measurements were performed at the Advanced Light Source to support these results (experimental details are described elsewhere [12]). The Pu $O_{4,5}$ XAS absorption edges ($5d \rightarrow 5f$) for α-Pu and δ-Pu in Fig. 3(a) are quite similar to the HE-EELS edges reported in Fig. 1. The similarity between HE-EELS and XAS can be further confirmed by comparing our U and Th HE-EELS to the

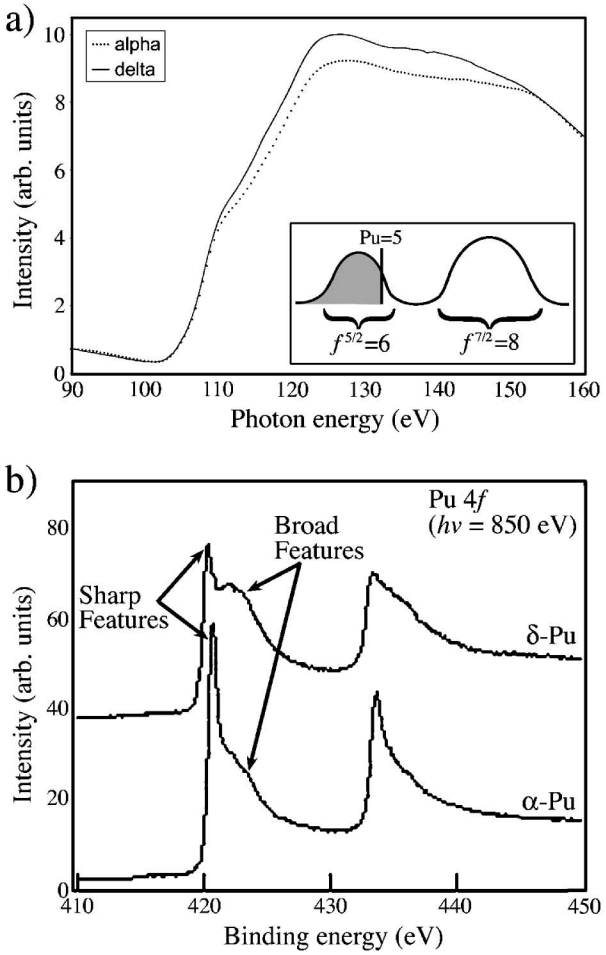

FIG. 3. (a) The $O_{4,5}$ ($5d \rightarrow 5f$) absorption edges from α-Pu and δ-Pu acquired by XAS using synchrotron radiation. (b) Core-level photoemission spectra from a large polycrystalline δ-Pu sample and a polycrystalline α-Pu sample. These spectra were collected with a photon energy of 850 eV, an analyzer pass energy of 6 eV, and an energy resolution of 0.2 eV.

XAS of α-Th by Aono *et al.* [13] and of α-U by Cukier *et al.* [14]. In both the HE-EELS and the XAS $O_{4,5}$ absorption edges of Th and U the prepeak is present. In the case of Pu, both the HE-EELS and the XAS of the Pu $5d \rightarrow 5f$ transition exhibit only the large continuum structure with no prepeak, a shift of approximately 1 eV between α-Pu and δ-Pu, and a peak leading edge in the region of 110 eV.

In the case of the XAS samples, *in situ* phase determination was made via the photoelectron spectroscopy of the Pu $4f$ levels, as shown in Fig. 3(b). The double component structure of each spin-orbit split peak, with a shoulder or broad maximum following the sharper line, has been shown previously [15] to be a reliable means of differentiating the α-Pu and δ-Pu phases. These XAS measurements were performed at a photon energy of $h\nu = 850$ eV and a kinetic energy of about 430 eV. Therefore, they are bulk sensitive with a mean free path of approximately 22 Å. Plutonium oxidizes notoriously fast, yet measured surface contamination due to O was small meaning the α-Pu and δ-Pu spectra were hardly influenced [12].

Now, let us return to reconsider the HE-EELS and XAS spectra in detail. The analogous transition in the rare earths is $4d^{10}4f^N \rightarrow 4d^9 4f^{N+1}$. For nearly all of the rare earth element series [16], the same $N_{4,5}$ spectral shape is observed: a sharp, prepeak structure at lower energies followed by a broad continuum peak at higher energies. This behavior has been explained previously by Dehmer *et al.* [17], Starace [18], and Sugar [19]. The Coulombic and exchange interactions between the partially occupied $4d$ and $4f$ final state levels drive the splitting of these angular-momentum-coupled states, generating energy splittings on the scale of 20 eV. The prepeak structure can persist as individual peaks, but at higher photon energies where the outgoing electron can actually escape, coupling to the continuum generates a large, broad peak that is often referred to as the giant resonance [20]. Sugar predicts that for $4f^{13}$, only a single line should be observed. The best observation of the end of series behavior is in Yb and YbO [21]. Yb ($4f^{14}$) shows no edge or line, but YbO ($4f^{13}$) exhibits a single, fairly broad peak. Thus, the characteristics of filling the rare earth $4f$ shell are the loss of prepeak structure at an initial state of $4f^{13}$ and the absence of any feature at an initial state of $4f^{14}$. If one applies this logic to Figs. 1 and 3(a), the conclusion is inescapable: In Pu the $5f^{5/2}$ level is being filled by the $5d^{10}(5f^{5/2})^5 \rightarrow 5d^9(5f^{5/2})^6$ transition. In the $4f$ levels of the lanthanides, the only filling effects that are observed are at the end of the series. (Half filling is possible but does not seem to be important: it may be obfuscated by the effects of multiple $4f$ valencies and interactions with the $5d6s$ manifold.) However, the data here show that in the actinides the filling can be seen to occur midseries, when the ($5f^{5/2}$) occupation goes from 5 to 6 in the process of XAS or HE-EELS [see the inset in Fig. 3(a)].

This interpretation is supported by several other pieces of experimental evidence. First, the prepeaks in Th and U are each singular and not particularly sharp. This is consistent with trends at the end of the rare earth series, not the beginning, where the prepeaks tend to be sharper and greater in number [16]. Second, the interpretation of the large broad peak with two steplike features on the low photon energy side in Pu as part of the metallic continuum structure is consistent with the observation and appearance of the M_2 and M_3 absorption edges in Ni [22] and the L_2 and L_3 edges in Al [23], which are examples of closely spaced edges in other metals. Third, the observation in the second case implies that the spin-orbit splitting of the initial states ($5d^{3/2}$ versus $5d^{5/2}$) should be reflected in the width of the giant resonance in Th, U, and Pu. In fact, this is observed: the giant

resonance becomes progressively wider in going from Th to U to Pu, where the value of the binding energy (BE) difference (BE $5d^{3/2}$ − BE $5d^{5/2}$) is 7.1, 8.6, and 12.4 eV, respectively [24]. Fourth, there is evidence that the filled $(5f^{5/2})^6$ exists in the Am ground state and affects its properties [25,26]. Fifth, other non-f systems have also exhibited evidence of the transition from LS to jj coupling [27,28].

This interpretation of $5f$ electronic structure has interesting implications. For example, it would explain the bremstrahlung isochromat spectroscopy (BIS) results of Baer and Lang for Th and U [29]. BIS can provide a measure of the unoccupied density of states above the Fermi level. Both U and Th exhibit a large, broad doublet in the BIS spectrum, with the larger peak at higher energy. In the Th spectrum ($5f^0$, Refs. [16,29]), the doublet is well above the Fermi energy, while in the U spectrum ($5f^3$, Refs. [16,29]), the low energy peak of the doublet is cut by the Fermi energy. The splitting between the doublet peaks is about 2 eV. An analysis of spin-orbit splitting in various series and levels predicts a spin-orbit splitting in the actinides $5f$ states of about 1 to 3 eV [30]. Our results substantiate the calculated $5f$ density of states of Th, U, α-Pu, δ-Pu, and Am by Pénicaud [26]. In Fig. 6 of Ref. [26] it is shown that the spin-orbit split $5f^{5/2} - 5f^{7/2}$ doublet for Th, U, α-Pu, and δ-Pu is approximately 2 eV, widens in energy with an increase in atomic number, and moves from the unoccupied states above the Fermi level to the occupied states below the Fermi level with an increase in atomic number. In both α-Pu and δ-Pu the $5f^{5/2}$ peak is almost entirely below the Fermi level while the $5f^{7/2}$ peak is above the Fermi level. Pénicaud's results also show that the filling of the $5f^{5/2}$ shell is progressive and is complete at Am. This is in contrast to the rare earths where because of the interaction of the $4f$ and $5d6s$ manifolds, the f states do not necessarily fill monotonically [16]. Our results also corroborate the viewpoint of Söderlind [31] that the upturn which occurs just before Pu in the graph of atomic volume versus atomic number is due to filling of antibonding states in the $5f^{5/2}$ subshell. Finally, and most importantly, these results confirm calculations that there is considerable spin-orbit splitting of the occupied and unoccupied $5f$ states of Pu, solidifying that spin-orbit splitting cannot be neglected in the Hamiltonian for the $5f$ states of Pu and the other actinides.

This work was performed under the auspices of the U.S. DOE by LLNL under Contract No. W-7405-Eng-48, with support from LANL (W-7405-ENG-36) and LBNL (BES, CSD, and ALS under DE-AC03-76SF00098). The ALS and beam line 7 have been built and operated under funding from the Office of Basic Energy Science at DOE. The authors thank Jason Lashley and Michael Blau for the Pu samples used at the ALS and J. Terry, J. D. Farr, T. Zocco, K. Heinzelman, and E. Rotenberg for help with the data collection at the ALS.

*Electronic address: moore78@llnl.gov

[1] R. C. Albers, Nature (London) **410**, 759 (2001).
[2] S. Y. Savrasov, G. Kotliar, and E. Abrahams, Nature (London) **410**, 793 (2001).
[3] S. Y. Savrasov and G. Kotliar, Phys. Rev. Lett. **84**, 3670 (2000).
[4] P. Söderlind, Europhys. Lett. **55**, 525 (2001).
[5] H. L. Skrivers, O. K. Andersen, and B. Johansson, Phys. Rev. Lett. **41**, 42 (1978).
[6] B. Johansson, Phys. Rev. B **11**, 2740 (1975).
[7] S. S. Hecker, D. R. Harbur, and T. G. Zocco, Prog. Mater. Sci. (to be published); *Challenges in Plutonium Science*, Los Alamos Science No. 26 (LANL, Los Alamos, NM, 2002), Vols. I, II.
[8] B. R. Cooper *et al.*, in *Handbook on the Physics and Chemistry of the Actinides,* edited by A. J. Freeman and G. H. Lander (Elsevier Science, Amsterdam, 1985), Vol. 2.
[9] R. Eisberg and R. Resnick, *Quantum Physics* (John Wiley and Sons, New York, 1974).
[10] C. Kittel, *Introduction to Solid State Physics* (John Wiley and Sons, New York, 1976), 5th ed., p. 442.
[11] R. F. Egerton, *Electron Energy-Loss Spectroscopy in the Electron Microscope* (Plenum Press, New York, 1996), 2nd ed., p. 221.
[12] J. Terry *et al.*, Surf. Sci. **499**, L141 (2002).
[13] M. Aono *et al.*, Solid State Commun. **39**, 1057 (1981).
[14] M. Cukier *et al.*, J. Phys. (Paris), Lett. **39**, L315 (1978).
[15] L. Havela *et al.*, Phys. Rev. B **65**, 235118 (2002).
[16] *Electronic Structure of Solids: Photoemission Spectra and Related Data*, edited by A. Goldmann and E. Koch, Landolt-Bornstein Numerical Data and Functional Relationships in Science and Technology, Group III, Vol. 23 (Springer-Verlag, Berlin, 1994). For rare earths, see Subvolume 23a, Chap. 2.5 by W. D. Schneider. For actinides, see Subvolume 23b, Chap. 2.8 by J. R. Naegale.
[17] J. L. Dehmer *et al.*, Phys. Rev. Lett. **26**, 1521 (1971).
[18] A. F. Starace, Phys. Rev. B **5**, 1773 (1972).
[19] J. Sugar, Phys. Rev. B **5**, 1785 (1972).
[20] S. R. Mishra *et al.*, Phys. Rev. Lett. **81**, 1306 (1998).
[21] L. I. Johansson *et al.*, Phys. Rev. B **21**, 1408 (1980).
[22] M. R. Thuler, R. Benbow, and Z. Hurych, Phys. Rev. B **27**, 2082 (1983).
[23] T. C. Chiang and D. E. Eastman, Phys. Rev. B **23**, 6836 (1981).
[24] R. Baptist *et al.*, J. Phys. F **12**, 2103 (1982).
[25] J. R. Naegele *et al.*, Phys. Rev. Lett. **52**, 1834 (1984).
[26] M. Pénicaud, J. Phys. Condens. Matter **9**, 6341 (1997).
[27] S. Mannervik *et al.*, Phys. Rev. Lett. **81**, 313 (1998).
[28] A. A. Wills *et al.*, Phys. Rev. Lett. **80**, 5085 (1998).
[29] Y. Baer and J. K. Lang, Phys. Rev. B **21**, 2060 (1980).
[30] J. G. Tobin (private communication).
[31] P. Söderlind, Ph.D. thesis, Uppsala University, 1994, p. 83.